

## INTEGRATED ULTRASONIC TRANSDUCER

Richard M. White, Sze-Hon Kwan, Kent Chuang, Richard S. Muller  
Department of Electrical Engineering and Computer Science  
and Electronics Research Laboratory  
University of California, Berkeley, California 94720

### ABSTRACT

The typical transducer considered consists of a piezoelectric film, and associated electrodes, connected to one gate of a dual-gate field-effect transistor in the silicon wafer on which the piezoelectric film is situated. An individual transducer responds to various modes of excitation (flexural, surface, bulk) at frequencies which may range from far below one Hertz to hundreds of megahertz. The second gate of the field-effect transistor can be used for electrical amplitude control or for mixing purposes. Connection of a number of these small transducers together to form arrays permits realizing ultrasonic receiving devices having variable directivity, and programmable surface-wave signal processors.

The transducer structures considered are shown in cross section in Fig. 1 (the vertical scale is exaggerated) with schematic symbols for easy representation. In the PI-DMOS transducer a single-gate field-effect transistor has a piezoelectric ZnO film deposited in the gate region on top of a thermally-grown SiO<sub>2</sub> layer. In the lower structure a commercial dual-gate double-diffused MOS transistor has one gate connected to a deposited piezoelectric ZnO film. Figure 2 shows the four modes of excitation of this transducer. Some waveforms appear in Fig. 3.

### THE INDIVIDUAL TRANSDUCER

Upon comparing the two transducer structures, one notes that the PI-DMOST structure offers both piezoelectric and pyroelectric response down to zero frequency owing to isolation of the ZnO film by high-quality thermally-grown SiO<sub>2</sub>. Fabrication of the second transducer structure is safer as no sputtering in the gate region is required. The second structure offers additional design freedom in the shaping of the piezoelectric region (hence control of directivity) and in its area for control of transducer sensitivity.

Response of PI-DMOST and the dual-gate sensor to application of static strain in a cantilever fixture (Fig. 4). At top, voltage across load resistance decreased as source-drain current dropped when strain was applied and remained at constant value for duration of test, 17.8 hours, after which it returned to original value. Lower scope trace shows that no dc response is observed with the second structure in which the ZnO film is not isolated by thermally-grown SiO<sub>2</sub>. It appears possible to provide such isolation with the dual-gate sensor if desired.

In Figs. 5-7 temperature sensitivity and dimensional design criteria are given.

### ELECTRICAL CONTROL OF TRANSDUCER

In the PI-DMOST a voltage may be applied externally to the gate, and in the dual-gate transducer (second structure) one may utilize the second gate to control the response to a signal applied via the piezoelectric film connected to the first gate. The amplitude of response can be adjusted with a control voltage V<sub>G2</sub>. Sampling of a low frequency output can be achieved by means of sampling pulses of short duration. Mixing in the dual-

gate transistor is achieved by application of a local oscillator signal at the second gate. In signal-processing arrays based on use of a number of these transducers, separate piezoelectric films could drive first and second gates to provide nonlinear coupling of different input signals.

### TRANSVERSAL FILTER SIGNAL PROCESSOR

Dual-gate transducers can be connected in an array to form a transversal filter structure as shown in Fig. 11. Although dependence of transducer amplitude upon second gate bias is nonlinear over part of its range (Fig. 12), by differencing two such transistor outputs a highly linear dependence of amplitude or tap weight upon bias is obtained, simplifying setting of tap weights (Fig. 13). An array processor operating near 27 MHz is being fabricated at present. Arrays of these transducers with second-gate control of weighting also appear attractive for use as ultrasonic receiving (and perhaps also transmitting) devices for scanning in defect characterization.

### SUMMARY

The integrated transducers based on use of a piezoelectric film and field-effect transistor are versatile devices offering

- response to various modes of excitation
- wide frequency response from dc if desired to hundreds of megahertz
- useful electronic control within the transducer itself
- possibility of interconnection into arrays for signal processing and detection.

### ACKNOWLEDGMENT

Research sponsored by the National Science Foundation Grant ENG76-21818 and the Center for Advanced NDE operated by the Science Center, Rockwell International, for the Advanced Research Projects Agency and the Air Force Materials Laboratory Contract F33615-74-C-5180.

### REFERENCES

- "Detection of Acoustic Waves with a PI-DMOST Transducer," K. W. Yeh, R. S. Muller, S. H. Kwan, Proc. 8th Conference (1976 International) on Solid State Devices, Tokyo, 1976, Jap. J. Appl. Phys. 16, Supplement, 16-1, 527-521 (1977).
- "Integrated Ultrasonic Transducer," S. H. Kwan, R. M. White, R. S. Muller, Proc. 1977 IEEE Ultrasonics Symposium, 843-846.

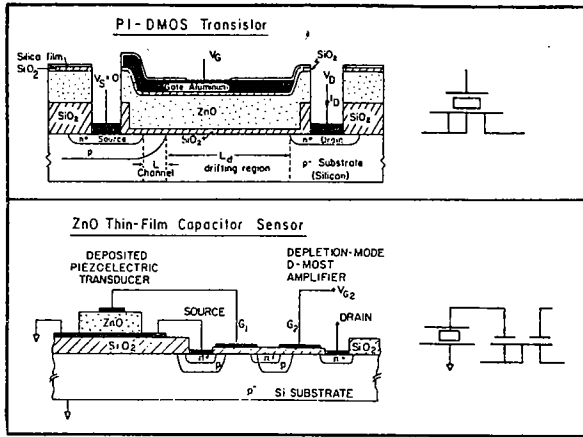


Fig. 1

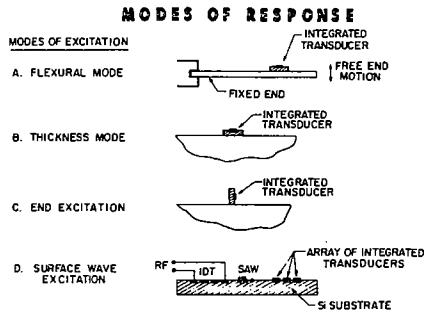


Fig. 2 Modes of excitation of the transducer. All four types of response have been observed experimentally, at frequencies ranging (for the PI-MOST structure) from less than one Hz in the flexural mode to about 90 MHz with surface acoustic wave excitation.

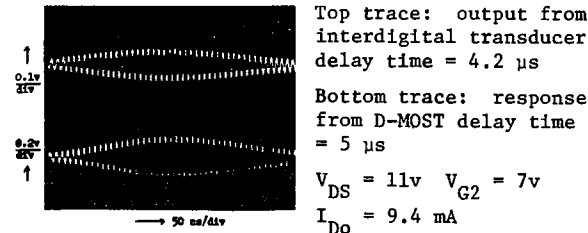
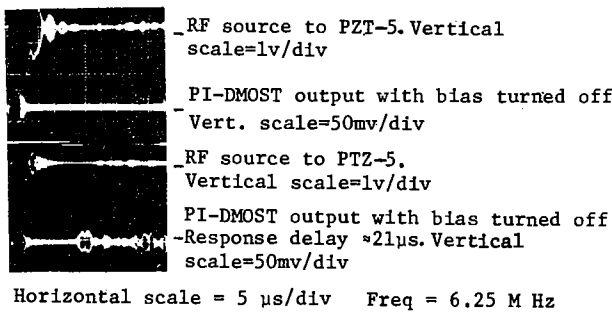
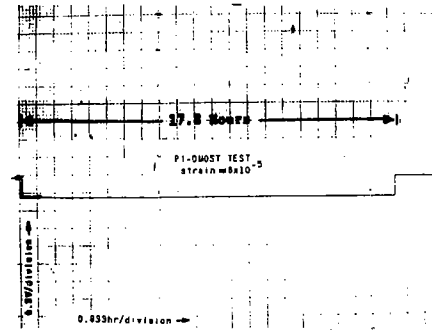


Fig. 3. Response of a PI-DMOST transducer (first structure) to bulk waves at 5 MHz and the ZnO dual-gate device (second structure) to SAW at 90 MHz. In latter, an output from an IDT on the same silicon wafer is shown for comparison.



2 sec/div

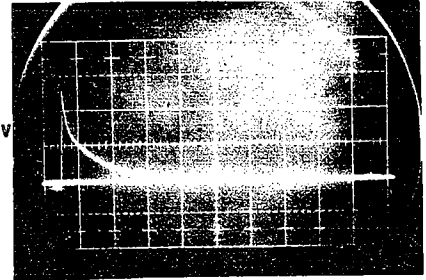
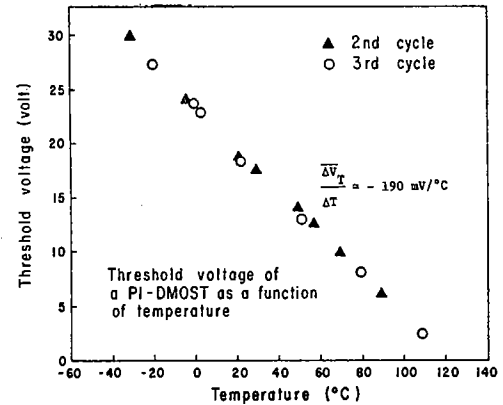


Fig. 4

Fig. 5 Temperature sensitivity of PI-DMOST. Owing chiefly to pyroelectric effect, threshold voltage changed each time temperature was altered and remained constant during the approximately 20 minutes of each step during which temperature was stable.



Calculated Temperature Dependence of Threshold Voltage for PI-DMOST Transducer

- (1) Pyroelectric effect in the ZnO layer

$$\frac{\Delta V_T}{\Delta T} = \frac{Q_{P1}}{C_{ZnO}} \approx -160 \text{ mV/}^\circ\text{C}$$

- (2) Thermal mismatching between the ZnO layer and the substrate

$$\frac{\Delta V_T}{T} = \frac{Q_{P2}}{C_{ZnO}} \approx -30 \text{ mV/}^\circ\text{C}$$

(3), Contribution from the Si substrate

$$\frac{\Delta V_T}{T} = -\frac{1}{T} \left\{ -\frac{E}{2} - |\phi_{fp}| \right\} \left\{ 1 - \frac{1}{C_0} \frac{Q_B}{2\phi_{fp}} \right\} \approx -10 \text{ mV}/^\circ\text{C}$$

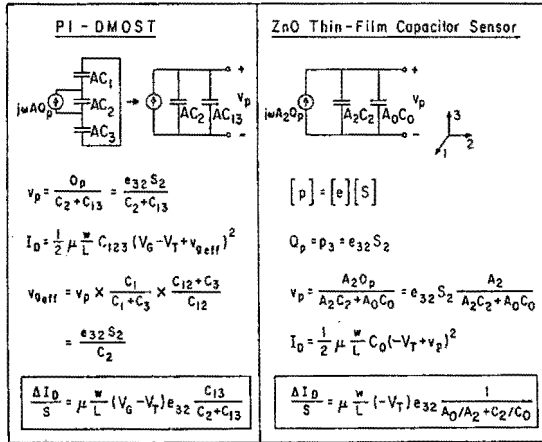


Fig. 6 Equivalent circuit models for the two transducer structures showing dependences upon area and capacitance per unit area ratios for ZnO (denoted 2), upper and lower oxides in PI-DMOST (1 and 3), and gate oxide in dual-gate DMOST (0).

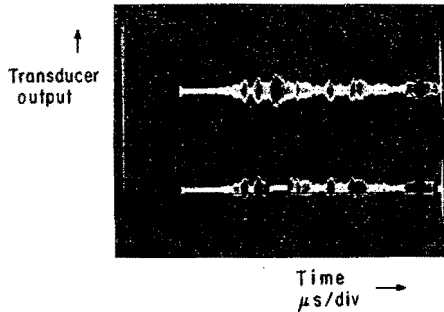


Fig. 8 **Amplitude Control.** Top trace of Fig. 8 shows output of dual-gate sensor in response to acoustic bulk longitudinal wave excitation at approximately 5 MHz with constant dc bias on second gate and signal applied to first gate. Lower trace shows effect of reduced gain near center of trace resulting from an 8 microsecond negative pulse superimposed on the dc second-gate bias. Such amplitude control could be used to deaden receiving transducer during "main bang" of nearby transmitting transducer or to select a portion of the output for display.

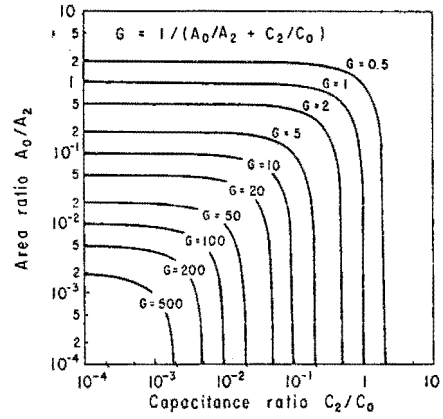


Fig. 7 Gain factor appearing in expression for sensitivity of second structure as function of area and specific capacity ratios. Typical transducer design would have gain factor ranging from 10 to 100.

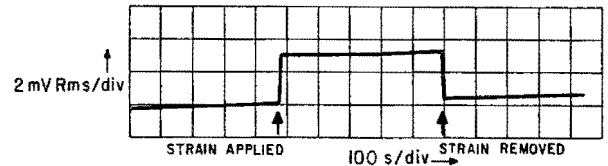
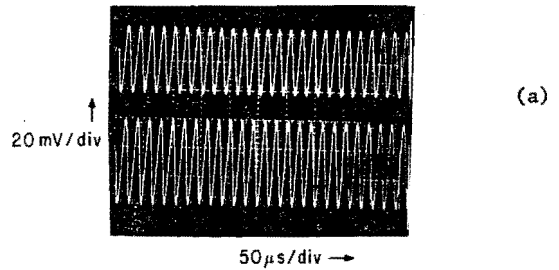
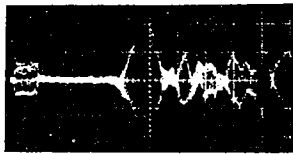


Fig. 9

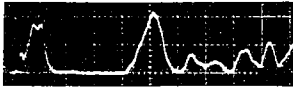
**Frequency Translation (Mixing).**

(A) **Frequency shifting with PI-DMOST.** In Fig. 9 50 kHz CW voltage was superimposed on the gate electrode of the first transducer structure during low-frequency strain measurements. Transducer output is at 50 kHz permitting use of lock-in detection and plotting on a chart recorder. Upper trace in photo shows output of transducer in non-strained state; lower trace shows output when strain is applied (roughly  $8 \times 10^{-5}$  strain magnitude). Portion of chart recording (Fig. 9b) shows corresponding output of lock-in amplifier (shift in baseline is believed due to drift of ions in gate oxide under influence of dc gate bias).

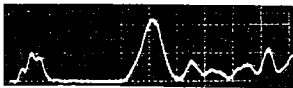
(B) **Mixing in dual-gate transducer (Fig. 10).** With signal on first gate the application of a local oscillator signal at second gate can produce mixing in the integrated transducer itself and output at an intermediate frequency. Maximum sum or difference output is observed when dc second-gate bias is adjusted for maximum rate of change of transconductance with second-gate bias voltage.



OUTPUT DISPLAYED DIRECTLY (NO LOCAL OSCILLATOR ON SECOND GATE) IN RESPONSE TO 5.5 MHz COMPRESSIONAL WAVE EXCITATION. 1 $\mu$ S/DIV. HORIZONTAL SCALE.



MIXING IN DUAL-GATE TRANSUDER. LOCAL OSCILLATOR 23.8 MHz. OUTPUT OF 30 MHz IF AMPLIFIER WITH DETECTOR.



MIXING IN DUAL-GATE TRANSUDER. LOCAL OSCILLATOR 35.2 MHz. OUTPUT OF 30 MHz IF AMPLIFIER WITH DETECTOR.

Fig. 10

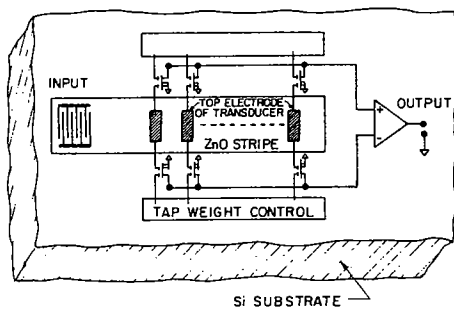


Fig. 11 Arrangement of transducers in differencing circuit to form SAW transversal filter processor. Outputs of the individual taps, the ZnO stripes with their electrodes, are amplified by controlled amounts by dual-gate transistors whose gains are set by the tap-weight block. Entire device could be integrated on a single silicon wafer. Bias circuitry is not shown.

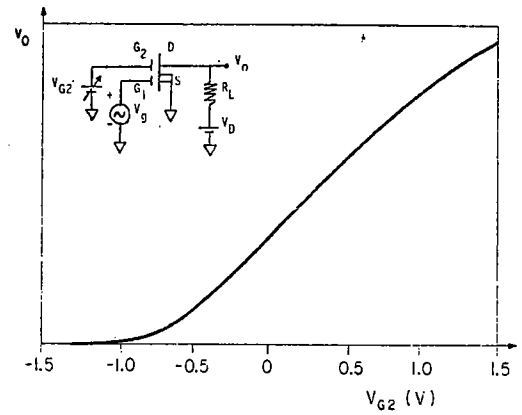


Fig. 12 Dependence of gain of a single dual-gate transistor upon control gate bias voltage  $V_{G2}$ .

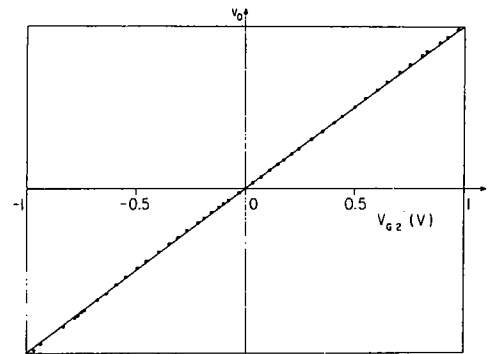


Fig. 13 Results of test of a simulated single tap in differencing scheme. Control biases of equal and opposite value were applied to two dual-gate transistors connected to differential amplifier. Analysis of result shows output is linear to within  $\pm 1$  db over a 51 db range.